FINITE ELEMENT SIMULATION OF HEAT TRANSFER IN FRICTION STIR WELDING OF Al 7050

E. Gharibshahiyan[1*] and A. Honarbakhsh Raouf[2]

* *gharibshahian@gmail.com*

Received: January 2016 Accepted: November 2016

[1] School of Materials Science and Metallurgical Engineering, Semnan University - R&D Department, Oghab Afshan Industrial & Manufacturing Company, Semnan, Iran.

[2] School of Materials Science and Metallurgical Engineering, Semnan University, Semnan, Iran.

Abstract: *Friction welding is widely used in various industries. In friction welding, heat is generated by conversion of mechanical energy into thermal energy at the interface the work pieces during pin rotation under pressure.*

A three-dimensional thermo mechanical simulation of friction stir welding (FSW) processes is carried out for Aluminium Alloys of 6061and 7050 where the simulation results are compared directly with the measured temperature histories during FSW after process.

The objective of the present work is to study and predict the heat transient generated in alloy aluminium plate welded by FSW method. A three dimensional model was developed by LS-Dyna software and heat cycles have been proposed during the welding of aluminium alloys 6061 and 7050.

In this research, the simulations were carried out with linear velocity in the range of 140 to 225 mm/min and pin rotational speeds of 390 and 500 rpm. Increase in pin rotational speed, from 390 to 500 rpm, resulted in greater temperatures which translated to rise of recorded temperature of top and bottom of the specimens. This is in turn to a wider HAZ. In addition, it was observed that raising the linear velocity had an opposite effect. Finally, results of experimental and numerical data were correlated and validated.

Keywords: *Friction stir welding (FSW), Aluminium alloy 6061 and 7050, Finite elements method.*

1. INTRODUCTION

Friction stir welding (FSW) is a new joining method derived from conventional friction welding which enables the advantages of solid state welding [1]. The FSW process is using a rotating cylindrical tool with a shoulder to generate frictional heat with a protruding smaller thread pin (or probe) that penetrates into and plasticizes the material in the vicinity of the joint line. The tool is plunged into and then traverses along the joint line along two butting work pieces. The advantages of this process include low residual stress, low energy input and a fine homogeneous microstructure compared to the conventional liquid–solid welding process [2].

Although it is a new welding technology, the FSW has been extensively studied in both academic and industrial communities for most aluminium alloys including difficult-to-weld alloys such as AA2195 (with lithium) and AA7075 [1, 3]. Over the past 20 years, research has been conducted enabling the use of advanced analytical procedures to more accurately simulate the welding process. Due to the complexity of the physical processes involved in welding, however, simple mathematical solutions cannot address the practical manufacturing processes. Furthermore, it is also impossible for any experimental technique to obtain a complete mapping of the residual stress and distortion distribution in a general welded structure. Computational simulation thus plays an indispensable role in the integrity analysis of such welded structures [4]. Due to computational and cost limitations, the first step in applying a two-dimensional (2D) finite element analysis (FEA) to predict thermal profiles and residual stress in a weldment. In reality, the thermal and stress–strain responses of all weldments are Three-dimensional (3D). With recent advancements in computational power, FEA simulation of transient temperature and residual stresses in welding has gradually become feasible. Temperature measurement in FSW for the workpiece was performed by Tang et al. [5]. A simple model for the temperature

[DOI: 10.22068/ijmse.13.4.53]

distribution in the workpiece was proposed by Gould and Feng [6]. Chao and Qi [7, 8] developed a moving heat source model in a finite element analysis for studying the temperature, residual stress and distortion of the FSW process. Furthermore, Colegrove et al. [9] and Frigaard et al. [10] developed three-dimensional heat flow models for the prediction of temperature fields in the FSW. Midling [11], Russell and Sheercliff [12] investigated the effect of tool shoulder material and pin tool on heat input during the FSW. Most currently, Donne et al. [13] reported the measured residual stresses in friction stir welds for 2024-T3 and 6013-T6 aluminium. Dong et al. [14] carried out a coupled thermo-mechanical analysis of the FSW process using a simplified two-dimensional axisymmetric model. Chao et al. [15] investigated the variations of heat energy and temperature produced by the FSW in both the workpiece and the pin tool. All investigations show that the FSW process of aluminium alloys yield welds with low distortion, high quality and low cost. Consequently, better structural performance is the primary advantage of this technology's applications. For example, a demonstration of the tremendous potential and successful applications of aluminium FSW in airframe structures can be found in Talwar et al. work [16]. Khandkar et al [17] represented an entrance coupling based on a model for Aluminium 6061-T6 friction weld.

In this study a three dimensional model have been used. To predict weld heat distribution of Al 7050 aluminium alloy 6061 was used as a base[18] to compare of former papers which expressed before this. The simulation method can be compared to practical data resulted from pervious papers report. To simulate the process and parameters in this study LS Dyna software was used [19]. The parameters being studied were welding tools liner velocity and rotary pin speed and finally temperature of the work piece.

2. EXPERIMENTAL PROCEDURE (MODEL)

In order to validate the results from the simulation of welding process, the model carried out by Khandkar [18] was employed. Experimental samples used for validation were two Aluminium 6061 plates having dimensions of 305×1058 mm each. A welding tool with shoulder diameter of 25 mm having a pin diameter of 10 mm was used. Pin length was 8 mm and its rotational speed was 390 rpm. The

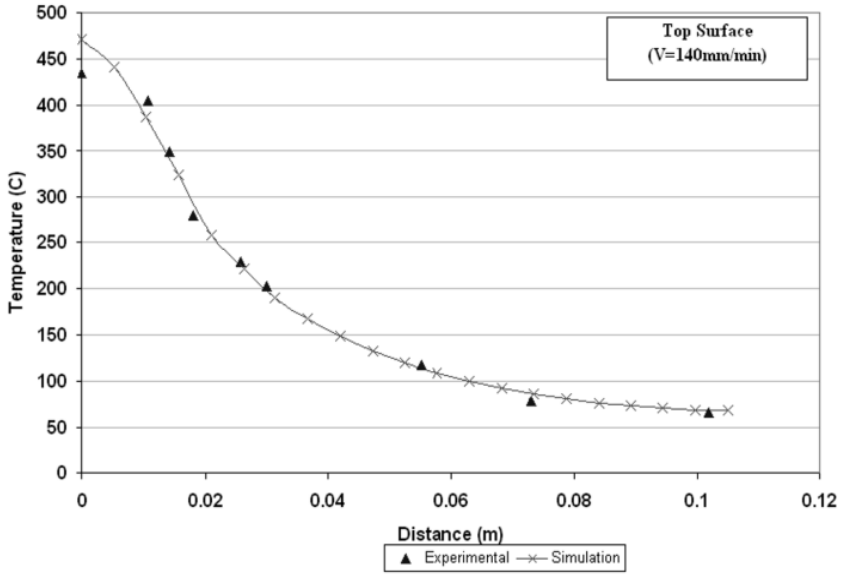

Fig. 1. Comparison between experimental and simulation data

[DOI: 10.22068/ijmse.13.4.53]

Table 1. Experimental and calculated test results and the amount of error at 190 mm from the weld

a. Temperature gradient at top of the specimen

	Weld line	15 mm	18 mm	26 mm	30 mm	55 mm	73 mm
Experimental test ºC	434	348	279	229	203	118	79
Simulation ºC	471	336	282	222	197	113	74
% Error	8.2	3.4	1	3	2.9	4.2	6.3

b. Temperature gradient at the bottom of specimen

	Weld line	15 mm	18 mm	26 mm	30 mm	55 mm	73 mm
Experimental test ºC	406	329	269	219	194	104	70
Simulation ºC	430	319	275	216	193	103	73
% Error	5.9	3	2.2	1.3	0.5	0.9	4.2

downward welding force and the linear tool movement were kept constant at 22.4 KN and 140 mm/min respectively.

Temperature gradients had been measured using 25 thermocouples located on different points. Figure (1) presents both experimental and numeral data resulted from simulation at a distance of 190 mm perpendicular to the weld line.

Table 1 shows the percentage of error between experimental and theoretical simulation indicating that maximum temperature produced on the surface of work piece in simulation model was 471 ºC which had about 37 degrees deviation from the practical test. Maximum temperature at the edge of the plates in simulated model was 74 ºC and it differs from physical test by 5 degrees. Further study of the graph shows an exceptional similarity in trend of in both numeral and experimental results. However, there is a small inconsistency at about 10 to 30mm distance from the weld line between practical test and computer simulation, which can be attributed to the performance of thermocouples.

It can be deduced from Table 1 that a good conformity in temperature gradient exists. This model was used to determine other parameters such as pin motion.

3. RESULTS AND DISCUSSIONS

Based upon verification between physical and simulation experiments conducted on Aluminium alloy 6061, various parameters such as linear velocity and pin rotational speed were changed and then Aluminium Alloy 7050 specimen was simulated. The linear velocity of tools during the welding is adjusted to keep the work piece under the melting point. Figure 2 and 3 illustrates the temperature maps of specimens after welding at 140 mm/min and pin rotational speed of 390 rpm for aluminium alloy 7050.

The temperature rise due to frictional force was calculated based on Fourier Equation.

In Equation 1, q, is the heat created by welding tool in contact with the surface of the specimen, Ω, is the material volume, and T, K, ρ and c are temperature, coefficient of thermal conductivity,

$$\rho c \frac{\partial T}{\partial x} = \frac{\partial}{\partial x} k_x \left(\frac{\partial T}{\partial x}\right) + \frac{\partial}{\partial y} k_y \left(\frac{\partial T}{\partial y}\right) + \frac{\partial}{\partial z} k_z \left(\frac{\partial T}{\partial z}\right) + q \; in \; \Omega \quad (1)$$

[DOI: 10.22068/ijmse.13.4.53]

$$q = \int_0^{R_0} 2\pi r^2 \mu(T)P(T)dr = {}^{2}/_{3}\,\pi\omega\mu(T)P(T)(R_0^3 - r_0^3) \quad (2)$$

material density and thermal capacity respectively.

The generated heat rate due to friction can be given by Equation 2.

R_0 and r_0 are radii of shoulder and pin respectively. Rate of heat generation between the shoulder and the upper surface of the work piece, is a function of the coefficient of friction μ (T),

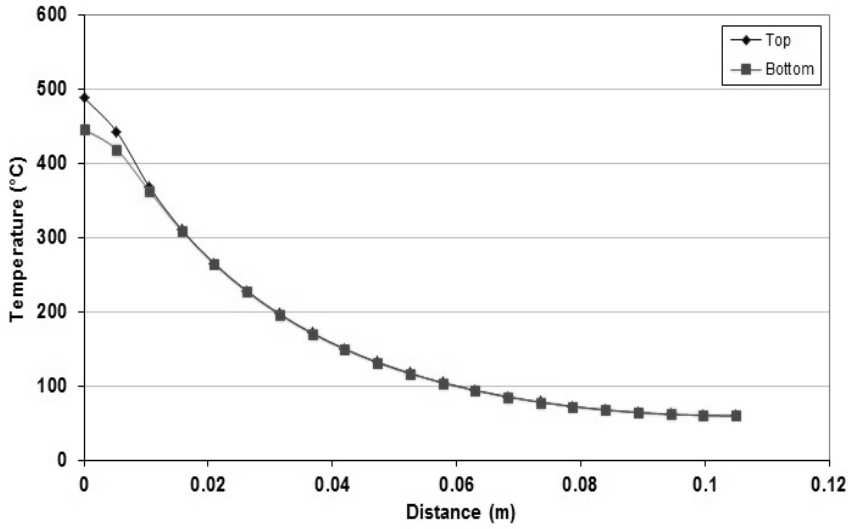

Fig. 2. Top surface temperature contours after 81.5 seconds at tool travel of 390 mm/min.

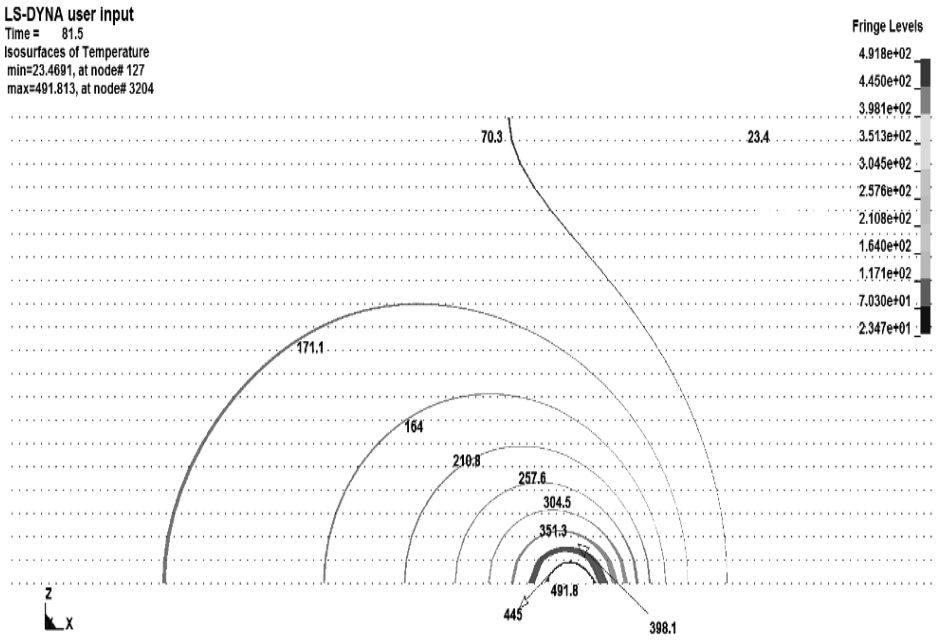

Fig. 3. Isothermal contours through the weld seam after 81.5 seconds at tool travel of 140 mm/min

[DOI: 10.22068/ijmse.13.4.53]

Fig. 4. a) Temperature profile at linear speed of 140 mm/min and rotational speed of 390 rpm, perpendicular to welding path b) Temperature profile at linear speed of 200 mm/min and rotational speed of 390 rpm, perpendicular to welding path

rotational speed ω and radius r. Where μ(T) and P (T) are coefficient of friction between welding tool and material and pressure of welding tool on surface of work piece respectively.

It would be difficult to evaluate the amount of μ (T) and P (T) from Equation 2. In this model a constant value for the coefficient of friction was considered to cover the effect of both the heat produced by friction and plastic deformation.

Figures 4 and 5 illustrate the welding temperature profile under various tool speeds at a distance of 190 mm perpendicular to the welding path.

Distribution of temperature in figure 4 shows, which curve of temperature, is a closer match to the actual FSW process. Raising the welding

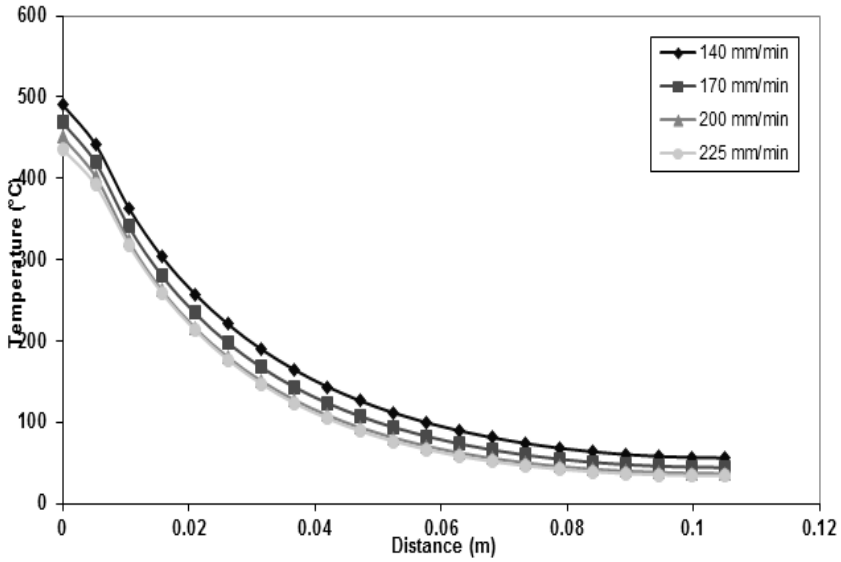

Fig. 5. Temperature gradient of the work piece as a function of linear pin speed for 390 rpm

[DOI: 10.22068/ijmse.13.4.53]

speed from 140 to 200 mm/min led to the weld line temperature drop from 488 °C to 450 °C (Figures 7,8), while the temperature distribution was identical in both cases. It can therefore be deduced that any changes in tool's linear speed does not affect the temperature distribution.

It can be observed from Figure 5 that maximum welding temperature of 490 °C was achieved at 140 mm/min and 390 rpm. As expected, this occurred at low linear tool speeds. The range of temperature at the edge of the plate was from 56 to 34 °C.

As expected, lowering the linear speed of the tool increased the contact time of the pin and shoulder with the work piece. This phenomenon led to a temperature rise of about 15% by reducing the linear speed from 200 to 90 mm/min (see Table 2).

In addition Table 2 shows that the temperature difference between the top and the bottom surfaces at constant tool rotational speed while varying linear speeds did not change and remained constant. This difference was 41 °C and 42 °C for linear speeds of 140 and 200 mm/min implying close temperature differences between top and bottom surfaces.

An increase in the rotational speed from 390 to 500 rpm, led to a jump in the welding temperature by 50 degrees (Figure 6).

Table 2. Peak temperatures obtained from simulation of FSW process for Al7050 alloy.

alloy	Rotational %elocity (rpm)	Liner %elocity (mm/min)	Top Surface Peak Temperature (°C)	Bottom Surface Peak Temperature (°C)
7050	390	140	448	445
		170	469	421
		200	456	404
		225	436	395
6061	390	140	471	430
		170	458	414
		200	438	396

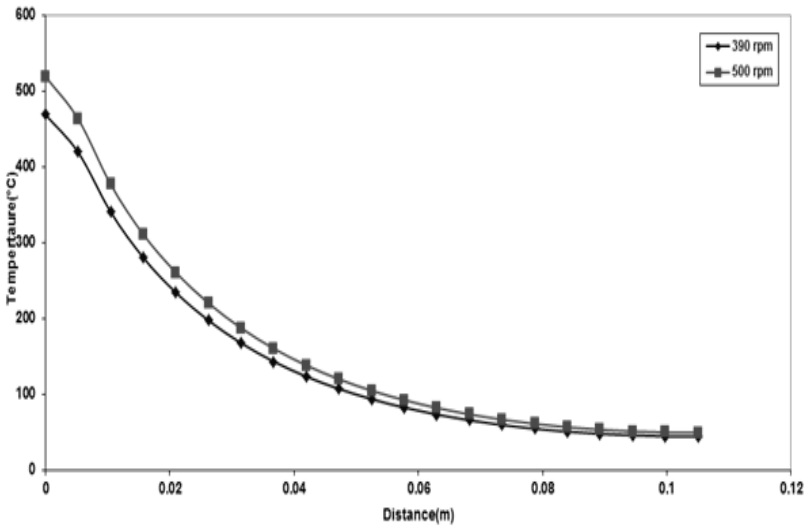

Fig. 6. Temperature distribution as a function of tool rotational speed at a constant linear tool speed of 170 mm/min

[DOI: 10.22068/ijmse.13.4.53]

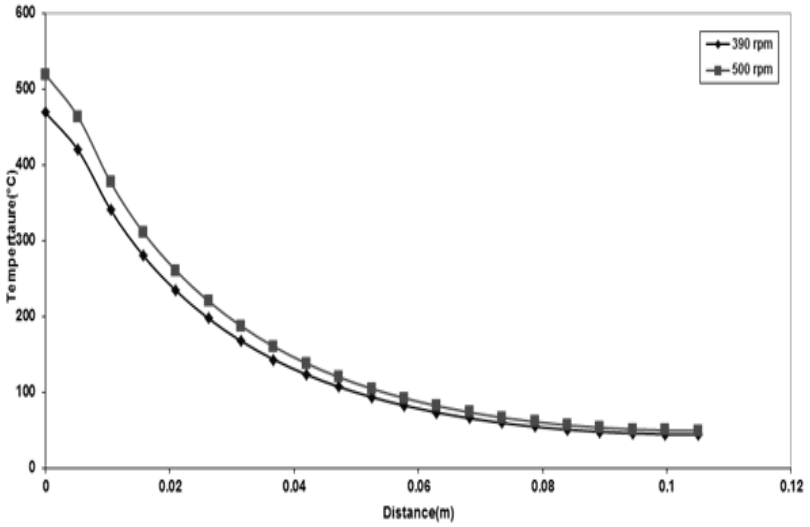

Fig. 7. Compare between temperature peaks calculated during FSW process.

Temperature rise (q), due to a high rotational speed can be explained by Equation 2. Practically, elevation of rotational speed from 390 to 500 rpm led to a temperature rise of 10.2%.

In figure 7 peak temperatures at weld centre line and distances away from it are shown with rotational speeds of 390 and 500 rpm while keeping the linear speed constant at 170 mm/min.

It can be seen in fig 7 that an increase in maximum weld temperature near the centre line is associates with the rise in rotational velocity.

One of the prominent characteristics of friction stir welding process is the redistribution of temperature near the weld line where residual stresses and distortion caused by the thermal stress are reduced.

4. CONCLUSIONS

In this study, the simulation of temperature distribution of a 7050 and 6061 Aluminium plates were performed and verified under experimental conditions, and the following conclusions were be deduced:

1. The numerically determined temperature fields matched extremely well with the experimental data. The maximum temperature during the FSW was at the weld line and it was about 471 °C to 436.
2. Reduction of linear tool velocity resulted in high welding temperature, so that the peak welding temperature of 471°C was recorded at a linear velocity of 140 mm/min.
3. A constant temperature difference between the two surfaces of the specimens was recorded under various processing parameters.

ACKNOWLEDGMENT

The authors would like to thank the Managing Director of Oghab Afshan Industrial & Manufacturing Company for financial support of this study.

REFERENCES

1. Zhu.X.K, Chao.Y.J, “Numerical simulation of transient temperature and residual stresses in friction stir welding of 304L stainless steel”, Journal of Materials Processing Technology, 2004,146, 263–272.
2. Cho. H.H, Kang. S.H, Kim. S. H, Oh. K. H, Ju. K. H, Chang. W. S, Han. H N, “Microstructural evolution in friction stir welding of high-strength linepipe steel”, Materials and Design

[DOI: 10.22068/ijmse.13.4.53]

2012, 34, 258–267.
3. Esmaily, M. and Shokuhfar, A., “Numerical simulation of heat transfer in friction stir welding of 7075-T6 aluminum alloy”, Mat.-wiss. u.Werkstofftech, 2010, 41, 350-355.
4. Alfaro, I., Racineux, G., Poitou, A., Cueto, E. and Chinesta, F., “Numerical simulation of friction stir welding by natural element methods”, Int J Mater Form, 2009, 2,225–234
5. Tang, W., Guo, X., McClure, J. C., Murr, L. E., Nunes, A., “Heat input and temperature distribution in friction stir welding”, J. Mater. Process. Manuf. Sci., 1998, 7, 163–172.
6. Gould, J., Feng, Z., “Heat flow model for friction stir welding of aluminum alloys”, J. Mater. Process. Manuf. Sci., 1998, 7, 185–194.
7. Chao, Y. J., Qi, X., “Thermal and thermo-mechanical modeling of friction stir welding of aluminum alloy 6061-T6”, J. Mater. Process. Manuf. Sci., 1998, 7, 215–233.
8. Chao, Y. J., Qi, X., “Heat transfer and thermo-mechanical modeling of friction stir joining of AA6061-T6 plates”, in: Proceedings of the First International Symposium on Friction Stir Welding, Thousand Oaks, CA, USA, 1999.
9. Colegrove, P., Pinter, M., Graham, D., Miller, T., “Three dimensional flow and thermal modelling of the friction stir welding process”, in: Proceedings of the Second International Symposium on Friction Stir Welding, Gothenburg, Sweden, June 26–28, 2000.
10. Frigaard, O., Grong, O., Midling, O. T., “A process model for friction stir welding of age hardening aluminum alloys”, Metal. Mater. Transition A, 2001, 32, 1189–1200.
11. Midling, O. T., “Effect of tool shoulder material on heat input during friction stir welding”, in: Proceedings of the First International Symposium on Friction Stir Welding, Thousands Oaks, CA, USA, June 14–16, 1999.
12. Russell, M. J., Sheercliff, H. R., “Analytic modelling of microstructure development in friction stir welding”, in: Proceedings of the First International Symposium on Friction Stir Welding, Thousands Oaks, CA, USA, June 14–16, 1999.
13. Donne, C. D, Lima, E., Wegener, J., Pyzalla, A., Buslaps, T., “Investigations on residual stresses in friction stir welds”, in: Proceedings of the Third International Symposium on Friction Stir Welding, Kobe, Japan, September, 2001, 27–28.
14. Dong, P., Lu, F., Hong, J. K. and Cao, Z., “Coupled thermomechanical analysis of friction stir welding process using simplified models”, Sci. Technol. Weld. Jointing, 2001, 6281–287.
15. Chao, Y. J., Qi, X., Tang, W., “Heat transfer in friction stir welding—experimental and numerical studies”, ASME J. Manuf. Sci. Eng., 2003, 125, 138–145.
16. Talwar, R., Bolser, B., Lederich, R., Baumann, J., “Friction stir welding of airframe structures”, in: Proceedings of the Second International Symposium on Friction Stir Welding, Gothenburg, Sweden, June 26–28, 2000.
17. Khandkar, M. Z. H, ‘‘Thermo-mechanical Modeling of Friction Stir Welding", PhD Dissertation, University of South Carolina, 2005.
18. Khandkar, M. Z. H., Khan, J. A., Reynolds, A. P., "Thermal Model of Friction Stir Welding of Al-6061", Trends in welding research, Proccedings of the 6th International Conference, Callaway Gardens Resort, Phoenix, Arizona, 2002, pp218-223. [19]. LS-DYNA Theory Manual, version 971, John O. Hallquiest , 2006.

[DOI: 10.22068/ijmse.13.4.53]